

# Measurements of the effective cumulative fission yields of $^{143}\text{Nd}$ , $^{145}\text{Nd}$ , $^{146}\text{Nd}$ , $^{148}\text{Nd}$ and $^{150}\text{Nd}$ for $^{235}\text{U}$ in the PHENIX fast reactor

Edwin Privas<sup>1</sup>, Gilles Noguere<sup>1,\*</sup>, Jean Tommasi<sup>1</sup>, Cyrille De Saint Jean<sup>1</sup>, Karl-Heinz Schmidt<sup>2</sup>, and Robert Mills<sup>3</sup>

<sup>1</sup> CEA, DEN Cadarache, 13108 Saint Paul Les Durance, France

<sup>2</sup> Centre d'Etudes Nucléaires Bordeaux Gradignan, CNRS/IN2P3, Univ. Bordeaux 1, 33175 Gradignan, France

<sup>3</sup> National Nuclear Laboratory, B170 Sellafield Works, Seascale, Cumbria CA20 1PG, UK

Received: 8 March 2016 / Received in final form: 13 June 2016 / Accepted: 20 June 2016

**Abstract.** The effective Neodymium cumulative fission yields for  $^{235}\text{U}$  have been measured in the fast reactor PHENIX relatively to the  $^{235}\text{U}$  fission cross-section. The data were derived from isotope-ratio measurements obtained in the frame of the PROFIL-1, PROFIL-2A and PROFIL-2B programs. The interpretations of the experimental programs were performed with the ERANOS code in association with the Joint Evaluated Fission and Fusion library JEFF-3.1.1. Final results for  $^{143}\text{Nd}$ ,  $^{145}\text{Nd}$ ,  $^{146}\text{Nd}$ ,  $^{148}\text{Nd}$  and  $^{150}\text{Nd}$  were 5.61%, 3.70%, 2.83%, 1.64% and 0.66%, respectively. The relative uncertainties attached to each of the cumulative fission yields lie between 2.1% and 2.4%. The main source of uncertainty is due to the fluence scaling procedure (<2%). The uncertainties on the Neodymium capture cross-sections provide a contribution lower than 1%. The energy dependence of the fission yields was studied with the GEF code from the thermal energy to 20 MeV. Neutron spectrum average corrections, deduced from GEF calculations, were applied to our effective fission yields with the aim of estimating fission yields at 400 keV and 500 keV, as given in the International Evaluated Nuclear Data Files (JEFF, ENDF/B and JENDL). The neutron spectrum average correction calculated for the PROFIL results remains lower than 1.5%.

## 1 Introduction

The present work reports experimental cumulative fission yields  $\bar{Y}_c(^A\text{Nd})$  that represent the total number of atoms of  $^A\text{Nd}$  produced over all time after one fission of  $^{235}\text{U}$  and averaged over the fast-neutron spectrum of the PHENIX reactor. Such experimental results are needed for the computer simulation of reactors, fuel cycles and waste management [1,2]. Values and relative uncertainties from current evaluations of interest for this work are listed in Table 1. A good knowledge of these quantities enables estimation of the spent fuel inventories and resultant quantities such as decay heat, delayed neutron and gamma ray emissions. They are also important in understanding fuel performance, such as reactivity loss during reactor operation. Apart from burnup and safety calculation, the isotope inventories can be used to characterize a spent fuel. The percentage burnup of actinide in the fuel can be determined by analyzing the fission product inventories. One of the fission yields routinely used for reactor applications is  $^{148}\text{Nd}$ . The burnup of fuel can be estimated using the stable

nuclide  $^{148}\text{Nd}$ , which is determined by destructive assay. The precursors of  $^{148}\text{Nd}$  are all short lived and have small cross-sections and thus the cumulative yield can be used to determine the number of fissions that has taken place in the fuel.

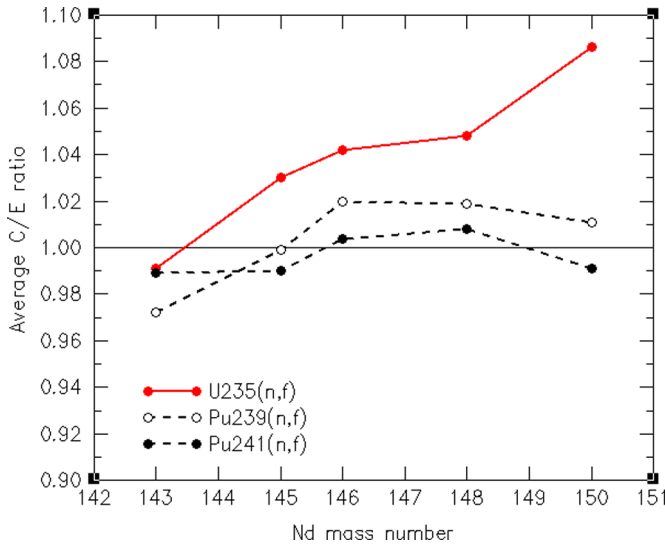
Previous interpretations of the PROFIL-1, PROFIL-2A and PROFIL-2B integral experiments carried out in the PHENIX reactor (CEA Marcoule, France) with the ERANOS code [6,7] in association with the evaluated nuclear data library JEFF-3.0 and JEFF-3.1 showed some significant discrepancies for the cumulative fission yields of several Neodymium isotopes for the fast fission of  $^{235}\text{U}$  [8,9]. The average calculated-to-experimental ratios  $C/E$  associated to the Neodymium produced by fission in several samples are gathered in Figure 1. Conspicuously, there is a large drift with respect to the atomic mass number  $A$  from  $A = 143$  to  $A = 150$ , far exceeding the claimed experimental uncertainties on fission yields, which lie in the range between 1% and 2.4%. Such a drift is not observed for the  $^{239}\text{Pu}$  and  $^{241}\text{Pu}$  samples.

A reanalysis of the PROFIL experiments was performed with the ERANOS code by using the nuclear data of the JEFF-3.1.1 library [5,10]. A similar drift of the average  $C/E$  values related to the Nd isotopes measured in the

\* e-mail: [gilles.noguere@cea.fr](mailto:gilles.noguere@cea.fr)

**Table 1.** Cumulative fission yields and relative uncertainties of  $^{143}\text{Nd}$ ,  $^{145}\text{Nd}$ ,  $^{146}\text{Nd}$ ,  $^{148}\text{Nd}$  and  $^{150}\text{Nd}$  for the fission of  $^{235}\text{U}$  in the fast-energy range recommended in the evaluated nuclear data libraries ENDF/B [3], JENDL [4] and JEFF [5].

Neodymium isotopes	ENDF/B-V11.1 500 keV	JEFF-3.1.1 400 keV	JENDL-4.0 500 keV
$^{143}\text{Nd}$	0.05731 (0.5%)	0.05533 (1.0%)	0.05722 (0.5%)
$^{145}\text{Nd}$	0.03776 (0.5%)	0.03797 (1.8%)	0.03768 (0.5%)
$^{146}\text{Nd}$	0.02921 (0.5%)	0.02927 (1.8%)	0.02917 (0.5%)
$^{148}\text{Nd}$	0.01683 (0.5%)	0.01697 (1.2%)	0.01680 (0.6%)
$^{150}\text{Nd}$	0.00686 (0.5%)	0.00702 (2.4%)	0.00685 (0.5%)

**Fig. 1.** Average  $C/E$  ratios for the prediction of the Neodymium buildup in the PROFIL-1 and PROFIL-2 programs for  $^{235}\text{U}$ ,  $^{239}\text{Pu}$  and  $^{241}\text{Pu}$  obtained with the ERANOS code and the JEFF-3.1 library [9].

$^{235}\text{U}$  samples was observed. This result confirms that the fast cumulative fission yields of the Nd isotopes recommended in the JEFF-3.1.1 library need to be revised with improved experimental values. The present work details how experimental fission yields with realistic uncertainties can be extracted from the integral trends provided by the PROFIL experiments. The originality of our data reduction and uncertainty analysis relies on the use of the Generalized Perturbation Theory [11], implemented in the ERANOS code, and of sensitivity coefficients calculated by direct perturbations of the nuclear data and experimental correction parameters.

The effective cumulative fission yields, given for the PHENIX neutron spectrum, were derived from the  $C/E$  values with an uncertainty lying between 2.1% and 2.4%. Special care was taken in evaluating the uncertainties related to the use of a new ERANOS calculation scheme in association with an improved fluence scaling procedure, needed to normalize the experimental results to the  $^{235}\text{U}$  fission cross-section. Biases caused by the Neodymium neutron capture reactions during irradiation were studied and quantified by direct perturbations of the capture cross-sections of the  $^{143}\text{Nd}$ ,  $^{145}\text{Nd}$ ,  $^{146}\text{Nd}$ ,  $^{148}\text{Nd}$  and  $^{150}\text{Nd}$

isotopes. Additional calculations performed with the GEF code [12,13] allowed accounting for the systematic behavior of the fission yields with the incident neutron energy. Final results are compared with experimental data reported in the literature and with evaluated data given at 400 keV or 500 keV in the JENDL, ENDF/B and JEFF nuclear data libraries.

## 2 Definition of the effective cumulative fission yields

A fission product is defined symbolically by the notation  $(A, Z, I)$  where  $A$  and  $Z$  are respectively the mass number and the atomic number, and  $I$  indicates the isomeric state. The ground state is denoted by  $I=0$  and  $I=1, 2, \dots$  represents the 1st, 2nd,  $\dots$  isomeric states. If a fission product has no isomers, or if one is referring to the sum of yields of all its isomers, the notation  $(A, Z)$  is used. Using this terminology, we can distinguish the independent and cumulative fission yields. For a given incident neutron energy  $E$ , the independent fission yield  $Y_{\text{post}}(A, Z, I, E)$  is the number of atoms of a specific nuclide produced directly per 100 fission reactions, after prompt neutrons evaporation but before any radioactive decay. To take into account radioactive decay, cumulative fission yield  $Y_c(A, Z, I, E)$  is used. It represents the number of atoms of a specific nuclide produced directly and via decay of precursors per 100 fission reactions. The cumulative fission yields can be defined by the expression [14]:

$$Y_c(A_i, Z_i, I_i, E) = Y_{\text{post}}(A_i, Z_i, I_i, E) + \sum_{j=0}^N Y_c(A_j, Z_j, I_j, E) b_{ji}(E), \quad (1)$$

where  $N$  is the dimension of the whole fission fragment inventory,  $i$  indicates a generic triplet  $(A_i, Z_i, I_i)$  and  $b_{ji}(E)$  is the branching ratio, which gives the probability that an isomer  $(A_j, Z_j, I_j)$  decays into  $(A_i, Z_i, I_i)$ .

In the present work, we report effective cumulative fission yields  $\bar{Y}_c$  measured in  $^{235}\text{U}$  samples, which have been irradiated in the fast reactor PHENIX. They can be obtained from:

$$\bar{Y}_c(A, Z, I) = \frac{\int_0^{E_{\text{max}}} Y_c(A, Z, I, E) \sigma_f(E) \varphi(E) dE}{\int_0^{E_{\text{max}}} \sigma_f(E) \varphi(E) dE}, \quad (2)$$

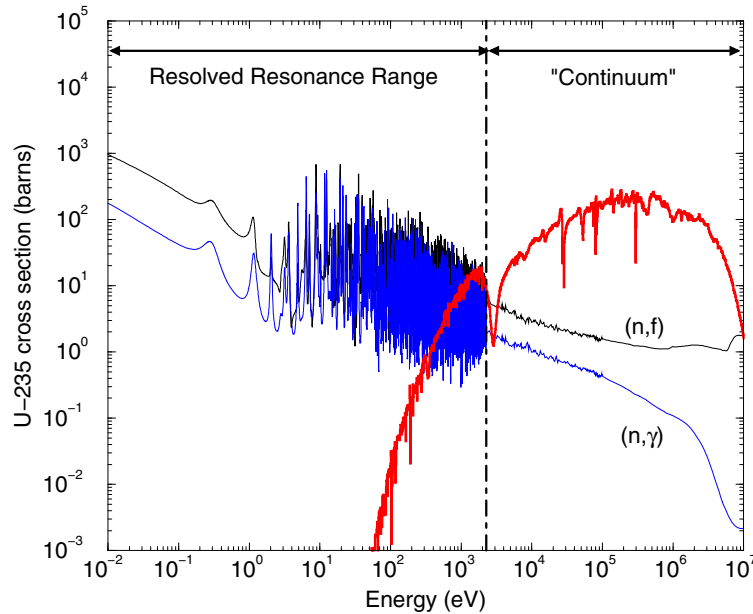


**Fig. 2.**  $^{235}\text{U}$  capture and fission cross-sections available in the JEFF-3.1.1 library compared to a neutron spectrum, in arbitrary unit, representative of the PROFIL experiment (red histogram).

in which  $\sigma_f(E)$  is the  $^{235}\text{U}$  fission cross-section and  $\varphi(E)$  stands for the fast-neutron spectrum representative of the PROFIL experiment. The maximum energy  $E_{\text{max}}$  is set to 20 MeV.

As stable Neodymium isotopes ( $Z=60$ ) in the ground state deformation ( $I=0$ ) are considered in this work, the notation  $Y_c(A, Z, I, E)$  and  $\bar{Y}_c(A, Z, I)$  will be replaced throughout the document by the explicit notation  $Y_c(^A\text{Nd}, E)$  and  $\bar{Y}_c(^A\text{Nd})$ .

### 3 Description of the PROFIL-1 and PROFIL-2 programs

The PROFIL programs were carried out in the fast reactor PHENIX (CEA Marcoule, France) from 1974 to 1980. They are mainly used to provide nuclear data feedbacks on neutron cross-sections ((n,γ), (n,2n), (n,f)) of several fission products and actinides. A detailed study of the integral results related to the cumulated fission yields of  $^{143}\text{Nd}$ ,  $^{145}\text{Nd}$ ,  $^{146}\text{Nd}$ ,  $^{148}\text{Nd}$  and  $^{150}\text{Nd}$  for  $^{235}\text{U}$  were never reported. The principle of the experimental setup is briefly described below. More information can be found in previous papers [8,9].

#### 3.1 Principle of the experiments

The PROFIL experiments were designed to study the fast energy range of the neutron cross-sections, called “continuum” in Figure 2. In the same figure, the  $^{235}\text{U}$  capture and fission cross-sections are compared to the fast-neutron spectrum calculated by using the ECCO lattice code of the ERANOS system [6,7] with 1968 energy groups and a critical buckling. Fission yields for the main actinides such as  $^{235}\text{U}$ ,  $^{238}\text{U}$ ,  $^{238}\text{Pu}$ ,  $^{239}\text{Pu}$ ,  $^{240}\text{Pu}$ ,

$^{241}\text{Pu}$ ,  $^{242}\text{Pu}$  and  $^{241}\text{Am}$  are also available. Only results obtained for the fission of  $^{235}\text{U}$  are presented in this paper.

The principle of the experiments consists of irradiating samples containing a small amount of pure isotope in a fast-neutron flux. The two experiments were carried out four decades ago during the first cycles of the 250 MWe sodium-cooled fast reactor PHENIX (CEA Marcoule, France). A simplified radial view of the core is presented in Figure 3. The first phase (PROFIL-1) was composed of a single experimental pin loaded in a standard PHENIX assembly placed at the center of the core. The pin contained 46 separate samples. The second phase (PROFIL-2A and PROFIL-2B) was a more ambitious program with two experimental pins, labelled A and B, placed in the inner core of PHENIX. Each pin contained 42 separate samples. Figure 3 also shows the pin location in their respective fuel subassemblies. A total of 130 samples were irradiated during four cycles for PROFIL-1 and PROFIL-2 (>10 months).

Samples loaded in the PROFIL pins were cylindrical containers with an outer diameter of 5.5 mm and a height of 8 mm. An example of a stainless steel double container is shown in Figure 3. For  $^{235}\text{U}$ , a total of 6 and 7 regularly spaced samples were loaded in the PROFIL-1 and in each PROFIL-2 pins, respectively. As shown in the axial layout of the PROFIL-1 pin (Fig. 4), the location of the  $^{235}\text{U}$  samples was chosen to provide accurate information for fluence scaling issue. We were able to use the experimental results of the 6 samples loaded in the PROFIL-1 pin, while only 3 samples (of the 7 samples) were analyzed in each PROFIL-2 pins. In total, up to 12 integral trends were collected for determining the cumulative fission yield of  $^{148}\text{Nd}$  and 9 integral trends for the other Neodymium isotopes.

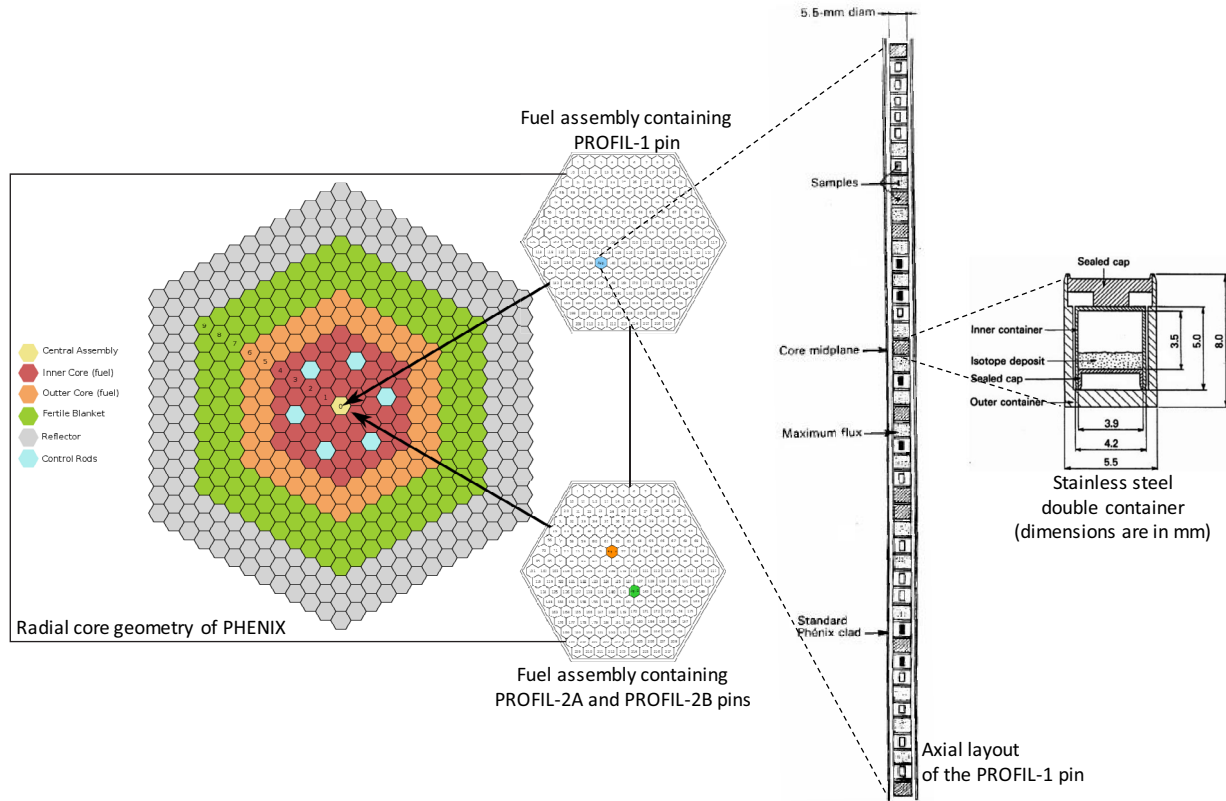


**Fig. 3.** Radial core geometry of the fast reactor PHENIX, location of the subassemblies containing the PROFIL pins, axial layout of the PROFIL-1 pin and example of a stainless steel double container designed for the PROFIL irradiation.

### 3.2 Isotope-ratio measurements

The experimental results used for the interpretation of the PROFIL experiments are the isotopic composition of the samples before and after the irradiation period. As indicated in Section 3.1, the time interval  $\delta t$  is of the order of 10 months. The variation, or equivalently the buildup, of the number of atoms provides integral information on the capture, fission and (n,2n) cross-sections.

We focus the present work on the isotopic composition of the  $^{235}\text{U}$  samples before and after the irradiation time  $\delta t$ . At the beginning of the experiment, the  $^{235}\text{U}$  samples are uranium oxide samples composed of  $^{235}\text{U}$  ( $\approx 90\%$ ),  $^{234}\text{U}$  ( $\approx 1\%$ ) and  $^{236}\text{U}$  ( $> 0.5\%$ ). After the irradiation period, we observe a decrease of  $\approx 20\%$  of the  $^{235}\text{U}$  content.

The determination of the sample composition was achieved by Inductively Coupled Plasma Mass Spectrometry (ICPMS) [15]. For each sample  $k$ , mass spectrometry measurements supplied high precision isotopic ratios ( $N_i^k/N_j^k$ ) whose relative uncertainties range from 0.1% to 0.2%. The variations  $\Delta(N_i^k/N_j^k)$  between  $t_0$  and  $t_0 + \delta t$  define the following experimental quantities:

$$E_{ij}^k(\delta t) = \Delta\left(\frac{N_i^k}{N_j^k}\right) = \frac{N_i^k(t_0 + \delta t)}{N_j^k(t_0 + \delta t)} - \frac{N_i^k(t_0)}{N_j^k(t_0)}. \quad (3)$$

Experimentally, the isotopic variations  $\Delta(N_{143\text{Nd}}^k/N_{148\text{Nd}}^k)$ ,  $\Delta(N_{145\text{Nd}}^k/N_{148\text{Nd}}^k)$ ,  $\Delta(N_{146\text{Nd}}^k/N_{148\text{Nd}}^k)$  and  $\Delta(N_{150\text{Nd}}^k/N_{148\text{Nd}}^k)$  have to be combined with the ratio  $\Delta(N_{148\text{Nd}}^k/N_{235\text{U}}^k)$  in order to deduce the isotopic variations of interest  $\Delta(N_{143\text{Nd}}^k/N_{235\text{U}}^k)$ ,  $\Delta(N_{145\text{Nd}}^k/N_{235\text{U}}^k)$ ,  $\Delta(N_{146\text{Nd}}^k/N_{235\text{U}}^k)$  and  $\Delta(N_{150\text{Nd}}^k/N_{235\text{U}}^k)$ . The corresponding values calculated with the ERANOS code are denoted by  $C_{ij}^k(\delta t)$ . Throughout the document, the C/E ratios have the generic form:

$$C/E \equiv C_{ij}^k(\delta t)/E_{ij}^k(\delta t). \quad (4)$$

In references [8,9], the quantities  $E_{ij}^k(\delta t)$  are assumed to be normally distributed and independent. As a consequence, the weighted average over the samples  $k$  of the calculated-to-experimental ratios, formally defined as:

$$\langle C/E \rangle \equiv \langle C_{ij}^k(\delta t)/E_{ij}^k(\delta t) \rangle, \quad (5)$$

are characterized by unrealistic small relative uncertainties. In practice, correlations between the uncertainties of the different ICPMS results were not provided by the experimentalists. Mathematical solutions to calculate appropriate uncertainties were discussed in reference [16] in which the experimental uncertainty on each isotopic

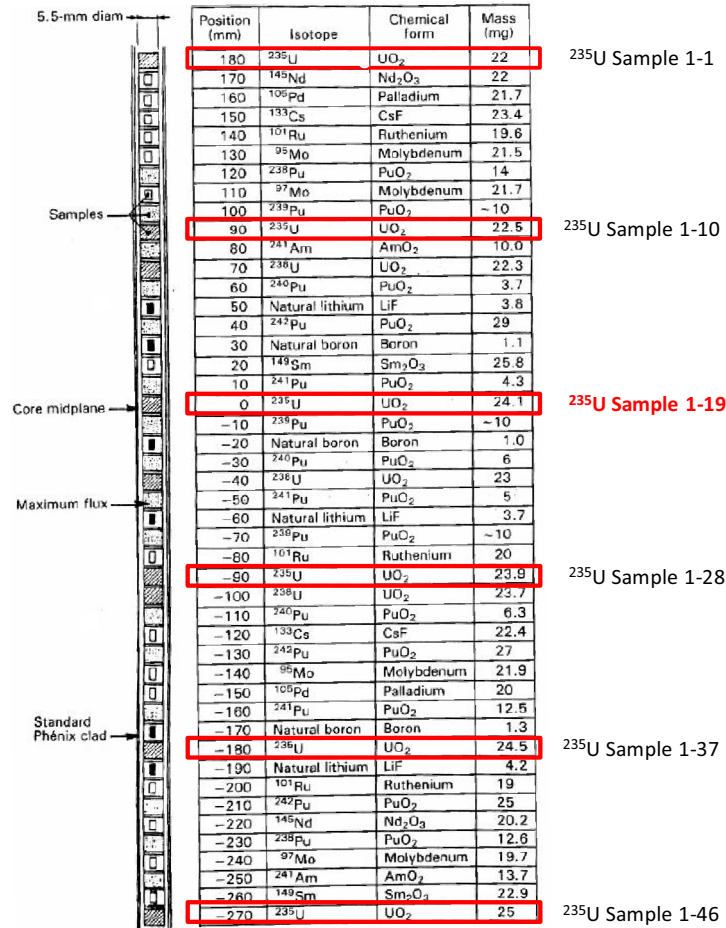


**Fig. 4.** Axial layout of the PROFIL-1 pin with the position of the <sup>235</sup>U samples used in this work. The sample number 19 is located at  $z = 0$  mm, which corresponds to the core midplane of the PHENIX reactor.

ratio is treated as a “statistical” contribution while the “systematic” part is driven by two fluence scaling parameters.

### 3.3 Fluence scaling issue

The interpretation of the PROFIL experiments is performed with the deterministic code ERANOS [6,7]. The calculation scheme relies on several hypotheses that are used to obtain a mean neutron flux over the irradiation period  $\delta t$ . The dispersion of the  $C/E$  ratios, observed for the <sup>235</sup>U samples, suggests that such a raw treatment overestimates the magnitude of the global fluence. The origins of the observed dispersions could be due to the approximations used in the calculation scheme but also to the influence of the surrounding materials, such as the steel containers, that could locally change the neutron spectrum. The strategy for solving the inconsistency between the calculations and the experimental results consists in normalizing the results utilizing the <sup>235</sup>U fission cross-section. For that purpose, two free parameters were introduced in the ERANOS calculations. The first parameter was introduced to shift the axial shape of the flux and the second parameter was introduced to normalize the global fluence level. Optimal parameter values are

determined by using as reference the following fission indicator:

$$E_{(235U+236U)238U}^k(\delta t) = \Delta \left( \frac{N_{235U}^k + N_{236U}^k}{N_{238U}^k} \right), \quad (6)$$

so that the related calculated-to-experimental ratios satisfy the following constraint:

$$\frac{C_{(235U+236U)238U}^k(\delta t)}{E_{(235U+236U)238U}^k(\delta t)} = 1. \quad (7)$$

For example, in the case of the PROFIL-2A configuration, the sensitivity of this experimental ratio to the <sup>235</sup>U fission cross-section is close to unity (1.07), whereas the sensitivity is relatively small to the <sup>238</sup>U capture cross-section (0.14) and negligible to the <sup>235,236</sup>U capture cross-sections (−0.04 and 0.01, respectively). The <sup>235</sup>U fission cross-section is one of the major reactions investigated within the “neutron cross-section standards” group of the International Atomic Energy Agency (IAEA) [17]. This cross-section is considered as a standard at thermal energy (25.3 meV) and from 0.15 MeV to

**Table 2.**  $C/E$  ratios for the prediction of the Neodymium buildup, after fluence scaling. Results obtained in the present work with the JEFF-3.1.1 library are compared with those obtained with the JEFF-3.1 library [18]. The 1st and 2nd weighted mean values for PROFIL were calculated with and without the  $C/E$  results obtained for the  $^{235}\text{U}$  sample number 19 located in the core midplane ( $z = 0$  mm). The quoted uncertainties are the experimental uncertainties coming from the chemical analysis of the  $^{235}\text{U}$  samples.

$^{235}\text{U}$ sample	Position (mm)	$^{143}\text{Nd}/^{235}\text{U}$			$^{145}\text{Nd}/^{235}\text{U}$			$^{146}\text{Nd}/^{235}\text{U}$			$^{148}\text{Nd}/^{235}\text{U}$			$^{150}\text{Nd}/^{235}\text{U}$		
		JEFF-3.1	JEFF-3.1.1	Exp. unc.	JEFF-3.1	JEFF-3.1.1	Exp. unc.	JEFF-3.1	JEFF-3.1.1	Exp. unc.	JEFF-3.1	JEFF-3.1.1	Exp. unc.	JEFF-3.1	JEFF-3.1.1	Exp. unc.
1-1	180	0.985	0.988	0.015	1.029	1.033	0.015	1.047	1.049	0.016	1.058	1.061	0.016	1.100	1.103	0.016
1-10	90	0.989	0.991	0.015	1.030	1.032	0.015	1.046	1.047	0.016	1.062	1.064	0.016	1.102	1.105	0.017
1-19	0	1.002	1.002	0.015	1.046	1.047	0.016	1.062	1.062	0.016	1.069	1.069	0.016	1.114	1.115	0.017
1-28	-90	0.992	0.992	0.015	1.030	1.030	0.015	1.044	1.044	0.016	1.057	1.057	0.016	1.102	1.102	0.017
1-37	-180	0.992	0.991	0.015	1.033	1.032	0.015	1.038	1.036	0.016	1.059	1.057	0.016	1.100	1.099	0.016
1-46	-270	0.990	0.987	0.015	1.031	1.029	0.015	1.031	1.028	0.015	1.055	1.052	0.016	1.097	1.095	0.016
1st weighted mean value		0.992	0.992	0.006	1.033	1.034	0.006	1.044	1.044	0.006	1.060	1.060	0.007	1.102	1.103	0.007
2nd weighted mean value		0.990	0.990	0.007	1.030	1.031	0.007	1.041	1.041	0.007	1.058	1.058	0.007	1.100	1.101	0.007
2-A08	130	0.985	0.982	0.005	1.021	1.018	0.005	1.035	1.031	0.006	1.040	1.036	0.005	1.061	1.058	0.006
2-A21	0	0.990	0.982	0.007	1.024	1.021	0.005	1.036	1.030	0.005	1.033	1.028	0.004	1.040	1.036	0.005
2-A35	-140										1.021	1.019	0.005			
Weighted mean value		0.986	0.982	0.004	1.023	1.020	0.004	1.036	1.030	0.004	1.032	1.026	0.003	1.049	1.045	0.004
2-B50	130										1.048	1.044	0.005			
2-B63	0	0.996	0.991	0.004	1.030	1.026	0.004	1.041	1.035	0.004	1.046	1.042	0.004	1.061	1.057	0.005
2-B70	-70										1.033	1.030	0.005			
Weighted mean value		0.996	0.991	0.004	1.030	1.026	0.004	1.041	1.035	0.004	1.043	1.039	0.003	1.061	1.057	0.005

200 MeV with relative uncertainties lower than 1%. Below 0.15 MeV, cross-section values reported by IAEA are given as a recommendation only. As calculated in reference [16], the accuracy of the fluence scaling, due to the precisions of the  $^{235}\text{U}$  fission cross-section, is close to 1.5% in average.

## 4 Integral results on Neodymium produced by fission

Integral results obtained from the interpretation of the PROFIL experiments with the ERANOS code are expressed in terms of calculated-to-experimental ratios (Eq. (4)), normalized to the  $^{235}\text{U}$  fission cross-section by using the fluence scaling operations shortly explained in Section 3.3. The main sources of uncertainties discussed in the following sections are the uncertainties related to (i) the calculation scheme, (ii) the calculation of the mean value (Eq. (5)), (iii) the calculation of the axial shape of the neutron flux, (iv) the fluence scaling and (v) the Nd capture cross-sections.

### 4.1 Calculated-to-experimental ratios obtained with JEFF-3.1.1

The  $C/E$  values obtained with the ERANOS code by using the JEFF-3.1 and JEFF-3.1.1 libraries are listed in Table 2 for each  $^{235}\text{U}$  sample. The two JEFF libraries share the same Nd cumulative fission yields [5]. The main difference between the two sets of results arises from the fluence scaling. In the previous calculations, the fluence scaling parameters (Sect. 3.3) were fine-tuned by trial and error. In the present work, their values were automatically adjusted so that the theoretical ratios of equation (6) agree with the experimental values within the limit of the uncertainties [16]. No significant differences are observed between the JEFF-3.1 and JEFF-3.1.1 results. The agreement lies between 0.1% and 0.5% for the PROFIL and PROFIL-2 results, respectively. A contribution of 0.5% will be added in the final uncertainty in order to account for the possible biases due to the calculation scheme.

The average ratios  $\langle C/E \rangle$  reported in Table 2 are displayed in Figure 5 as a function of the mass of the Neodymium isotopes. These results confirm the trends reported in the previous works (Fig. 1). A satisfactory agreement is observed between the two PROFIL-2 pins (A and B). The discrepancies range from 0.5% (for the  $^{145}\text{Nd}$  and  $^{146}\text{Nd}$  buildup) to 1.3% (for the  $^{148}\text{Nd}$  buildup). The main interesting result shown in Figure 5 is the sizeable difference between the PROFIL-1 and PROFIL-2 results in the case of the  $^{150}\text{Nd}$  buildup. The origin of such a difference is difficult to explain with the available experimental information.

### 4.2 Uncertainties on the average values

A closer inspection of the integral results has shown that the average values in the PROFIL-1 experiment are slightly dependent on the  $C/E$  values reported for the  $^{235}\text{U}$  sample number 19. This sample is located in the PROFIL-1 pin at

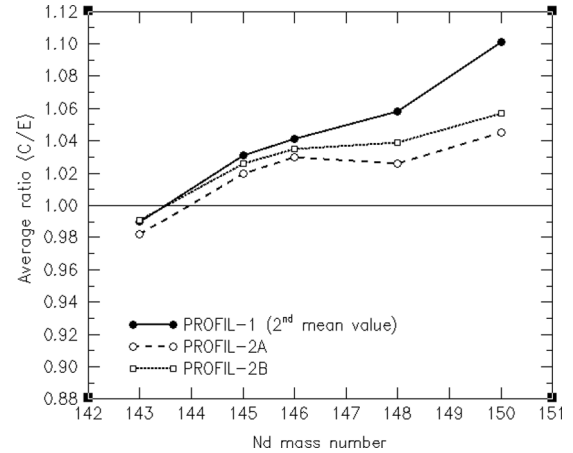


**Fig. 5.** Average  $\langle C/E \rangle$  ratios for the prediction of the Neodymium buildup in the PROFIL-1, PROFIL-2A and PROFIL-2B programs for  $^{235}\text{U}$  obtained with the ERANOS code and the JEFF-3.1.1 library. Individual results are listed in Table 2.

**Table 3.**  $C/E$  ratios for the prediction of the  $^{144}\text{Nd} + ^{144}\text{Ce}$  buildup in the  $^{235}\text{U}$  samples of the PROFIL pin, after fluence scaling. Results obtained in the present work with the JEFF-3.1.1 library are compared with those obtained with the JEFF-3.1 library [18].

$^{235}\text{U}$ sample	$(^{144}\text{Nd} + ^{144}\text{Ce})/^{235}\text{U}$		
	JEFF-3.1	JEFF-3.1.1	Exp. unc.
1-1	1.028	1.030	0.015
1-10	1.029	1.031	0.015
1-19	1.173	1.174	0.018
1-28	1.066	1.066	0.016
1-37	1.039	1.038	0.016
1-46	1.026	1.023	0.015

$z = 0$  mm, which corresponds to the core midplane of the PHENIX reactor (Fig. 4). As a complementary information, Table 3 reports the  $C/E$  values obtained for the  $^{144}\text{Nd} + ^{144}\text{Ce}$  buildup. Results found for the  $^{235}\text{U}$  sample number 19 are always significantly greater than the other  $^{235}\text{U}$  samples. A similar trend with a lower amplitude can be observed in the plots of Figure 6. They display the  $C/E$  ratios related to the prediction of the  $^{143}\text{Nd}$ ,  $^{144}\text{Nd} + ^{144}\text{Ce}$ ,  $^{145}\text{Nd}$ ,  $^{146}\text{Nd}$ ,  $^{148}\text{Nd}$  and  $^{150}\text{Nd}$  buildup in the  $^{235}\text{U}$  samples of the PROFIL-1 experiment as a function of the sample position in the pin. In each case, the highest value is reached at  $z = 0$  mm, which makes questionable the accuracy attached to the sample number 19. The average ratios  $\langle C/E \rangle$  calculated with and without the  $C/E$  results obtained for the  $^{235}\text{U}$  sample number 19 are reported in Table 2. The differences between the two sets of average values range from 0.2% to 0.3%. In the following, the 2nd set of mean values reported in Table 2 (ignoring the sample 19 results) will be considered for the determination of the cumulative fission yields. An additional uncertainty of 0.3%, associated to this choice, will be taken into account.

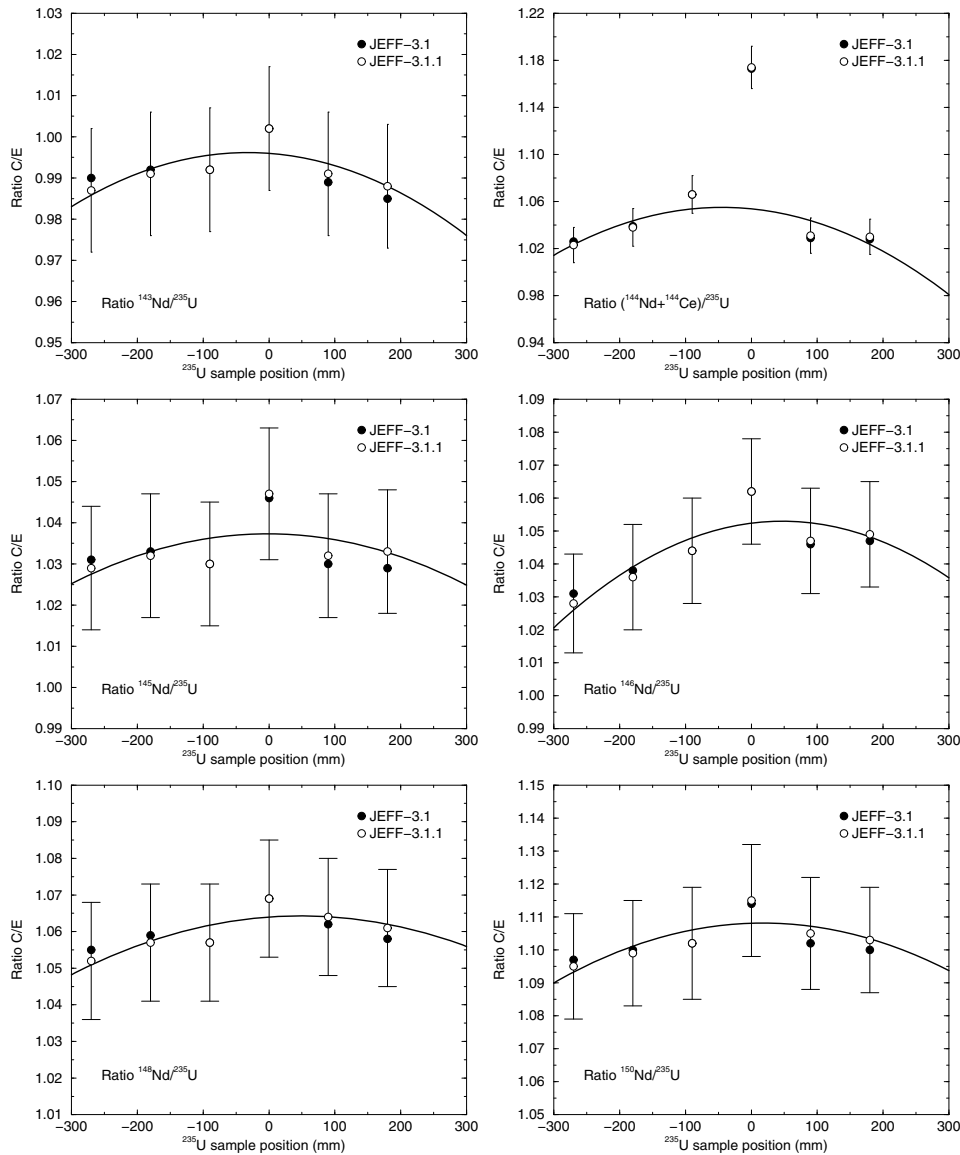


**Fig. 6.** Comparison of the individual  $C/E$  results obtained with JEFF-3.1.1 (open circle) and JEFF-3.1 (black circle) for the prediction of the  $^{143}\text{Nd}$ ,  $^{144}\text{Nd} + ^{144}\text{Ce}$ ,  $^{145}\text{Nd}$ ,  $^{146}\text{Nd}$ ,  $^{148}\text{Nd}$  and  $^{150}\text{Nd}$  buildup in the  $^{235}\text{U}$  samples of the PROFIL-1 experiment as a function of the sample position. The abscise  $z = 0$  mm corresponds to the core midplane of the PHENIX reactor. The solid line is a parabolic curve fitted to the data acting as a eye guide.

### 4.3 Uncertainties due to the axial shape of the neutron flux

A suspicious experimental trend can also be observed in Figure 6. In each plot, there is an apparent trend, fitted to a parabolic curve as an eye guide, with axial position. Such a behavior as a function of the sample position can be seen as a systematic trend between the middle and the extremity of the PROFIL pin, which is usually associated with the capability of our calculation scheme to correctly reproduce the axial shape of the neutron flux and the edge effects far away from the core midplane. This could be an explanation why the  $C/E$  results for the sample number 19 (located in the core midplane of the PHENIX reactor) are systematically higher (see Sect. 4.2). Full 4D Monte-Carlo simulations for correcting this trend were not investigated

in the present work. Instead, we introduce an additional source of uncertainty of 1% related to the axial shape of the neutron flux.

### 4.4 Uncertainties due to the fluence scaling

The recent work on the PROFIL programs reported in reference [16] shows that the uncertainties on the calculated isotopic ratio are dominated by the accuracy of the neutron fluence scaling close to  $\Delta\phi/\phi = 1.5\%$  on average. The corresponding uncertainty attached to the average  $\langle C/E \rangle$  values can be estimated with a sensitivity analysis.

The sensitivity  $S(\phi)$  of the calculated isotopic ratio to the fluence was established by direct perturbation of the 2nd scaling parameter, which normalizes the global fluence level (Sect. 3.3). Values of  $S(\phi)$  are reported in Table 4 and

**Table 4.** Mean sensitivity  $S(\phi)$  in %/% of the calculated Neodymium buildup in the  $^{235}\text{U}$  samples to the fluence [18]. The relative uncertainties  $(\Delta C/C)_\phi$  due to the accuracy of the neutron fluence scaling ( $\Delta\phi/\phi = 1.5\%$ ) is calculated with equation (8).

Isotopic ratio	PROFIL-1		PROFIL-2	
	$S(\phi)$	$(\Delta C/C)_\phi$	$S(\phi)$	$(\Delta C/C)_\phi$
$^{143}\text{Nd}/^{235}\text{U}$	1.11	1.7%	1.22	1.7%
$^{145}\text{Nd}/^{235}\text{U}$	1.10	1.7%	1.21	1.7%
$^{146}\text{Nd}/^{235}\text{U}$	1.15	1.7%	1.31	2.0%
$^{148}\text{Nd}/^{235}\text{U}$	1.12	1.7%	1.24	1.9%
$^{150}\text{Nd}/^{235}\text{U}$	1.12	1.7%	1.24	1.9%

result from the difference of two ERANOS calculations. The quoted uncertainties on the Neodymium ratios are the product of the sensitivity times the uncertainty associated to the fluence scaling:

$$\left(\frac{\Delta C}{C}\right)_\phi = S(\phi) \frac{\Delta\phi}{\phi}. \quad (8)$$

This sensitivity study demonstrates that no sizeable dependences of  $S(\phi)$  are observed between the different isotopic ratios. Therefore, an incorrect fluence scaling cannot explain the increasing bias with the Nd mass number shown in Figures 1 and 5.

#### 4.5 Uncertainties due to the Nd capture cross-sections

The final source of uncertainties investigated in this work is the contribution of the uncertainties of the Nd capture cross-sections to the calculated isotopic ratio.

Figure 7 compares the Nd capture cross-section available in the JEFF-3.1.1 library with a neutron spectrum representative of the PROFIL experiments. For the capture process, the fast-energy range of interest in the neutronic calculations lies between 1 keV and 1 MeV. The sensitivity is maximum around 30 keV. This energy also corresponds to the temperature relevant for the neutron capture nucleosynthesis. Improved compilation of  $(n,\gamma)$  reactions at  $kT = 30$  keV has been updated in order to provide a set of recommended Maxwellian Averaged Neutron Cross Section between 1 keV and 100 keV. Two sets of Nd neutron cross-sections published in 2000 and 2006, respectively are reported in Table 5. The recommended values are similar with slightly different uncertainties. We can observe large differences with the JEFF-3.1.1 neutron capture cross-sections ranging from 4% to 20%, far exceeding the uncertainties recommended in references [19,20]. The bias of 9% and 14% calculated for the  $^{143}\text{Nd}(n,\gamma)$  and  $^{145}\text{Nd}(n,\gamma)$  reactions, respectively, are consistent with the overestimation of 13% and 19% reported in the previous PROFIL interpretations [8,9].

The sensitivity  $S(\sigma_\gamma)$  of the calculated Neodymium buildup in the  $^{235}\text{U}$  samples to the Nd capture cross-sections are listed in Table 6. They were calculated with the perturbation formalism of the ERANOS code. The mathematical framework is detailed in reference [11]. Low

sensitivity coefficients are obtained because the Nd capture cross-sections in the fast-energy range remain lower than 1 barn. The negative impact of the  $^A\text{Nd}$  capture cross-section on the ratio  $^A\text{Nd}/^{235}\text{U}$  is associated to a positive impact of similar magnitude on the ratio  $^{A+1}\text{Nd}/^{235}\text{U}$ . Due to published data not included for the  $^{150}\text{Nd}(n,\gamma)$  reaction at 30 keV in the Atlas of Neutron Resonances [20], the recommendation of Bao et al. [19] were used to estimate the uncertainties reported in the last two columns of Table 6. The uncertainties attached to the Nd capture cross-sections and the bias between the JEFF-3.1.1 library and the recommended values are treated separately as follows:

$$\left(\frac{\Delta C}{C}\right)_{\text{unc}} = S(\sigma_\gamma) \left(\frac{\Delta\sigma_{\gamma\text{Bao}}}{\sigma_{\gamma\text{Bao}}}\right), \quad (9)$$

and

$$\left(\frac{\Delta C}{C}\right)_{\text{bias}} = S(\sigma_\gamma) \left(\frac{\sigma_{\gamma\text{JEFF}}}{\sigma_{\gamma\text{Bao}}} - 1\right). \quad (10)$$

The present results confirm the conclusions reported in reference [22], in which the author suggests that a global uncertainty lower than 1% could have resulted from omitting to make this correction for the Nd capture cross-sections.

## 5 Results and discussions

The experimental results provided by the PROFIL experiments are related to effective cumulated fission yields  $\bar{Y}_c(^A\text{Nd})$ , which are associated to a given neutron spectrum. Fast-reactor fission yields reported in the literature could have variations due to the neutron energy dependence of the fission yields. The GEF code [12,13] was used to study for this energy dependence and to extract preliminary trends on cumulated fission yields  $Y_c(^A\text{Nd}, E)$  at  $E = 400$  keV and  $E = 500$  keV.

### 5.1 Effective cumulative fission yields

The average calculated-to-experimental ratios  $\langle C/E \rangle$  listed in Table 2 for PROFIL-1, PROFIL-2A and PROFIL-2B (calculated with JEFF-3.1.1) are reported in Table 7 together with the sources of uncertainties discussed in

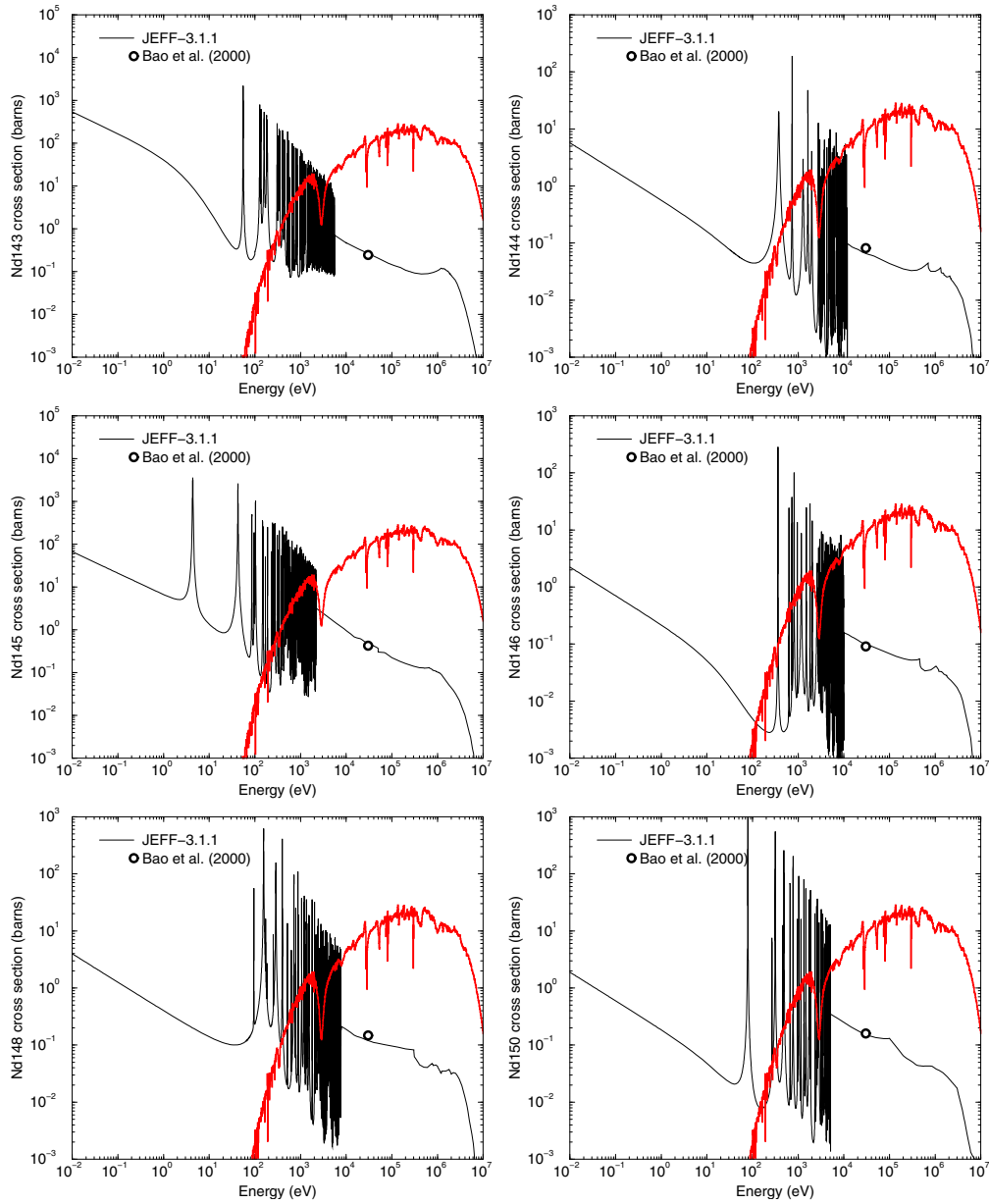


**Fig. 7.** Nd capture cross-sections available in the JEFF-3.1.1 library and recommended in reference [19] at 30 keV compared to a neutron spectrum, in arbitrary units, representative of the PROFIL experiments (red histogram).

**Table 5.** Comparison of the capture cross-section reported in references [19,20] and in the JEFF-3.1.1 library at 30 keV.

Neutron reaction	JEFF-3.1.1	Neutron cross-sections at $kT = 30$ keV		Ratios	
		$\sigma_{\gamma_{\text{Bao}}}$ [19]	$\sigma_{\gamma_{\text{Mug}}}$ [20]	$\sigma_{\gamma_{\text{JEFF}}}/\sigma_{\gamma_{\text{Bao}}}$	$\sigma_{\gamma_{\text{JEFF}}}/\sigma_{\gamma_{\text{Mug}}}$
$^{143}\text{Nd}(n,\gamma)$	266.8 mb	$245.0 \pm 3.0$ mb (1.2%)	$244.6 \pm 6.2$ mb (2.5%)	1.09	1.09
$^{144}\text{Nd}(n,\gamma)$	65.9 mb	$81.3 \pm 1.5$ mb (1.8%)	$82.8 \pm 1.4$ mb (1.7%)	0.81	0.80
$^{145}\text{Nd}(n,\gamma)$	485.7 mb	$425.0 \pm 5.0$ mb (1.2%)	$424.8 \pm 9.0$ mb (2.1%)	1.14	1.14
$^{146}\text{Nd}(n,\gamma)$	98.6 mb	$91.2 \pm 1.0$ mb (1.1%)	$91.2 \pm 2.0$ mb (2.2%)	1.08	1.08
$^{148}\text{Nd}(n,\gamma)$	120.0 mb	$147.0 \pm 2.0$ mb (1.4%)	$146.6 \pm 3.8$ mb (2.5%)	0.82	0.82
$^{150}\text{Nd}(n,\gamma)$	152.3 mb	$159.0 \pm 10.0$ mb (6.3%)		0.96	

**Table 6.** Sensitivity  $S(\sigma_\gamma)$  in %/% of the calculated Neodymium buildup in the  $^{235}\text{U}$  samples to the Nd capture cross-sections. The last two columns report the relative uncertainties calculated with equations (9) and (10) by using the relative uncertainties  $(\Delta\sigma_{\gamma_{\text{bao}}}/\sigma_{\gamma_{\text{bao}}})$  reported in reference [19] and ratios  $(\sigma_{\gamma_{\text{JEFF}}}/\sigma_{\gamma_{\text{Bao}}})$  given in Table 5.

Isotopic ratio	Sensitivity coefficients $S(\sigma_\gamma)$ (%/%)					Relative uncertainties		
	$\sigma_\gamma(^{143}\text{Nd})$	$\sigma_\gamma(^{144}\text{Nd})$	$\sigma_\gamma(^{145}\text{Nd})$	$\sigma_\gamma(^{146}\text{Nd})$	$\sigma_\gamma(^{148}\text{Nd})$	$\sigma_\gamma(^{150}\text{Nd})$	$(\Delta C/C)_{\text{unc}}$	$(\Delta C/C)_{\text{bias}}$
$^{143}\text{Nd}/^{235}\text{U}$	-0.013						0.02%	0.12%
$^{144}\text{Nd}/^{235}\text{U}$	0.015	-0.002					0.02%	0.17%
$^{145}\text{Nd}/^{235}\text{U}$		0.003	-0.043				0.06%	0.66%
$^{146}\text{Nd}/^{235}\text{U}$			0.051	-0.008			0.07%	0.78%
$^{148}\text{Nd}/^{235}\text{U}$					-0.013		0.02%	0.23%
$^{150}\text{Nd}/^{235}\text{U}$						-0.013	0.08%	0.05%

Sections 4.1–4.5. Their quadratic sum leads to overall relative uncertainties ranging from 2% to 2.5%, mainly dominated by the contribution of the fluence scaling uncertainty.

The uncertainty analysis, reported in Section 4, indicates that the main sources of uncertainties cannot alone explain the large drift on the calculated-to-experimental ratios with respect to the Nd mass number observed in Figures 1 and 5. As a consequence, we can expect that the observed discrepancies between the calculated and experimental values are mainly due to the Nd cumulative fission yields used in the ERANOS calculations. This statement has been verified with a sensitivity analysis.

The sensitivity coefficients  $S(\bar{Y}_c)$  of the average ratios  $\langle C/E \rangle$  to the effective Nd fission yields were estimated by a direct perturbation analysis. Results reported in Table 7 were calculated from the difference of two ERANOS calculations. They indicate that the  $S(\bar{Y}_c)$  values are of similar magnitude and close to 0.98, confirming the strong sensitivity of the calculated-to-experimental ratios to the Nd cumulative fission yields. Since the ERANOS calculations were performed by using the cumulative fission yields  $\bar{Y}_{\text{cJ}}(^A\text{Nd})$  of the JEFF-3.1.1 library, experimental values  $\bar{Y}_c(^A\text{Nd})$  can be determined as follows:

$$\bar{Y}_c(^A\text{Nd}) = \bar{Y}_{\text{cJ}}(^A\text{Nd}) + \Delta\bar{Y}_c(^A\text{Nd}), \quad (11)$$

where  $\Delta\bar{Y}_c(^A\text{Nd})$  is related to the average calculated-to-experimental ratios  $\langle C/E \rangle$  via the relationship:

$$\frac{\Delta\langle C/E \rangle}{\langle C/E \rangle} = S(\bar{Y}_c) \frac{\Delta\bar{Y}_c(^A\text{Nd})}{\bar{Y}_{\text{cJ}}(^A\text{Nd})}, \quad (12)$$

with the condition:

$$\langle C/E \rangle + \Delta\langle C/E \rangle = 1. \quad (13)$$

By introducing equations (12) and (13) in equation (11), we obtain:

$$\bar{Y}_c(^A\text{Nd}) = \left( 1 + \frac{1 - \langle C/E \rangle}{S(\bar{Y}_{\text{Nd}})\langle C/E \rangle} \right) \bar{Y}_{\text{cJ}}(^A\text{Nd}). \quad (14)$$

In the ERANOS calculations, we have to account for that the cumulative fission yields in the JEFF-3.1.1 library are given at three incident neutron energies (25.3 MeV, 400 KeV and 14 MeV). In absence of a fine description of the energy dependence of the cumulative fission yields, we always assume that:

$$\bar{Y}_{\text{cJ}}(^A\text{Nd}) = Y_{\text{cJ}}(^A\text{Nd}, E = 400 \text{ keV}), \quad (15)$$

where  $Y_{\text{cJ}}(^A\text{Nd}, E)$  represents the fast-cumulative fission yield of JEFF-3.1.1, reported in the 3rd column of Table 1. The final experimental values  $\bar{Y}_c(^A\text{Nd})$ , calculated with equation (14), are reported in Table 7. The mean values  $\langle \bar{Y}_c(^A\text{Nd}) \rangle$ , averaged over the PROFIL-1, PROFIL-2A and PROFIL-2B results, are given below:

$$\langle \bar{Y}_c(^{143}\text{Nd}) \rangle = 0.05605 \pm 0.00117 (2.1\%),$$

$$\langle \bar{Y}_c(^{145}\text{Nd}) \rangle = 0.03703 \pm 0.00083 (2.2\%),$$

$$\langle \bar{Y}_c(^{146}\text{Nd}) \rangle = 0.02826 \pm 0.00069 (2.4\%),$$

$$\langle \bar{Y}_c(^{148}\text{Nd}) \rangle = 0.01636 \pm 0.00037 (2.3\%),$$

$$\langle \bar{Y}_c(^{150}\text{Nd}) \rangle = 0.00660 \pm 0.00015 (2.3\%).$$

The obtained uncertainties were automatically calculated with the uncertainty propagation capabilities of the CONRAD code [21] by using the standard law:

$$\text{var}(\langle \bar{Y}_c(^A\text{Nd}) \rangle) = S_{\langle \bar{Y}_c \rangle} D S_{\langle \bar{Y}_c \rangle}^t, \quad (16)$$

in which  $S_{\langle \bar{Y}_c \rangle}$  represents the sensitivity matrix of  $\langle \bar{Y}_c(^A\text{Nd}) \rangle$  to the average ratios  $\langle C/E \rangle$  and  $D$  is the covariance matrix between the average ratios  $\langle C/E \rangle$ . The covariance matrix  $D$  can be separated in two parts to account for the statistical and systematic uncertainties listed in Table 7. The covariance matrix for the statistical part is a diagonal matrix, while the covariance matrix for the systematic part contains correlations close to unity, mainly because of the fluence scaling uncertainty.

**Table 7.** Summary of the weighted mean values  $\langle C/E \rangle$ , given in Table 2, and of the statistical and systematic uncertainties obtained for the PROFIL-1 (1), PROFIL-2A (2A) and PROFIL-2B (2B) experiments with the JEFF-3.1.1 library. The effective fission yields  $\bar{Y}_c(^4\text{Nd})$  were calculated with equation (14) and  $\langle \bar{Y}_c(^4\text{Nd}) \rangle$  are the average values calculated over the three PROFIL experiments.

Isotopic ratio	$^{143}\text{Nd}/^{235}\text{U}$		$^{145}\text{Nd}/^{235}\text{U}$		$^{146}\text{Nd}/^{235}\text{U}$		$^{148}\text{Nd}/^{235}\text{U}$		$^{150}\text{Nd}/^{235}\text{U}$			
	1	2A	2B	1	2A	2B	1	2A	2B	1	2A	2B
Average ratio $\langle C/E \rangle$	0.990	0.982	0.991	1.031	1.020	1.026	1.041	1.030	1.035	1.039	1.101	1.045
Statistical uncertainty	0.007	0.004	0.004	0.007	0.004	0.004	0.007	0.004	0.004	0.003	0.007	0.004
Systematic uncertainties												
Unc. mean value (%)	0.3			0.3			0.3				0.3	
Unc. calculation scheme (%)	0.5	0.5	0.5	0.5	0.5	0.5	0.5	0.5	0.5	0.5	0.5	0.5
Unc. axial flux (%)	1.0	1.0	1.0	1.0	1.0	1.0	1.0	1.0	1.0	1.0	1.0	1.0
Unc. fluence scaling (%)	1.7	1.7	1.7	1.7	1.7	1.7	1.7	2.0	2.0	1.9	1.7	1.9
Unc. capture cross-section (%)	0.1	0.1	0.1	0.7	0.7	0.7	0.9	0.9	0.9	0.3	0.1	0.1
Total systematic uncertainties (%)	2.1	2.0	2.0	2.2	2.2	2.2	2.2	2.5	2.5	2.2	2.1	2.2
Sensitivity coefficient $S(\bar{Y}_c)$ (%/%)	0.985	0.985	0.985	0.979	0.979	0.979	0.984	0.984	0.984	0.977	0.979	0.979
Effective fission yield $\bar{Y}_c(^4\text{Nd})$ (%)	5.589	5.634	5.583	3.676	3.719	3.696	2.805	2.837	2.823	1.652	0.630	0.662
Uncertainty (%)	2.2	2.0	2.0	2.3	2.2	2.2	2.3	2.5	2.5	2.3	2.2	2.3
Average effective fission yield $\langle \bar{Y}_c(^4\text{Nd}) \rangle$ (%)		5.605			3.703			2.826		1.636		0.660
Uncertainty (%)		2.1			2.2			2.4		2.3		2.3

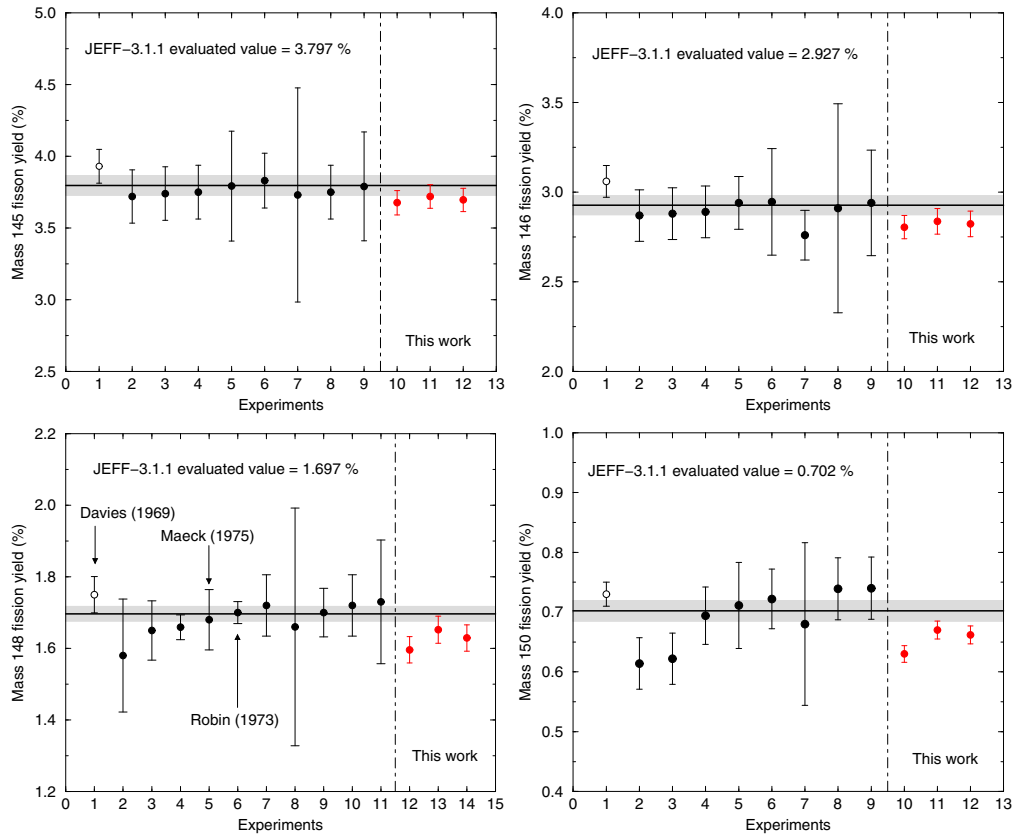


**Fig. 8.** Effective Nd cumulative fission yields obtained in this work (Tab. 7) compared to Experiments data used in the evaluation procedure of the JEFF-3.1.1 Fission Yield library.

## 5.2 Comparison with experimental data

Few sets of data are reported in the literature for fast-reactor conditions. The main experimental data of interest were measured in the DOUNREAY [22], EBR-I [23], RAPSODIE [24,25], EBR-II [26] and PROTEUS [27] fast reactors in the 70s. Figure 8 compares the PROFIL results with a selected set of data used in the evaluation procedure of the fission yields for the JEFF library [14]. For the  $^{145}\text{Nd}$  and  $^{146}\text{Nd}$  fission yields, our results agree with the data within the limit of the uncertainties. For the  $^{148}\text{Nd}$  and  $^{150}\text{Nd}$  fission yields, a larger spread between the data can be observed. We have focused our attention on the singular trends of the data reported for  $^{148}\text{Nd}$ .

In Figure 8, the 1st values in each plot (open circle) are the experimental fission yield of Davies [22] measured in the DOUNREAY reactor (Caithness, UK). The Davies' data are systematically higher. For  $^{148}\text{Nd}$ , the cumulative fission yield used in the evaluation procedure of JEFF is  $0.0175 \pm 0.0005$ . The low uncertainty of 3% has the consequence of increasing its weight on the evaluated yield value.

Robin et al. [24] also report a cumulated fission yield for  $^{148}\text{Nd}$  of 0.017 with a low uncertainty of 1.8% at  $2\sigma$ , in which systematic uncertainties are not included. The Robin's data come from the TACO experiment performed in the fast-neutron critical mock-up reactor RAPSODIE located in the CEA of Cadarache (France). TACO

provided useful technical knowledge for the design of the PROFIL programs in a power reactor. A dedicated analysis of the TACO results were performed by Koch [25] for establishing systematics of fast-cumulative fission yields. The analysis of two  $^{235}\text{U}$  samples lead to a cumulated fission yield for  $^{148}\text{Nd}$  of 0.01665, which is 2% lower than the Robin's value.

If realistic uncertainties are taken into account during the evaluation procedure, a cumulated fission yield for  $^{148}\text{Nd}$  close to 0.0168 is expected. This value is fully consistent with the experimental result of  $0.0168 \pm 0.0002$  reported by Maeck in 1975 [26]. Unfortunately, in 1981, Maeck et al. published revised and updated fast-reactor fission yields and indicated that these data superseded earlier values from EBR-II published in 1975 [28], making questionable any average values that include results coming from EBR-II. The discussion of the uncertainties, proposed in this work, demonstrates the difficulty for assessing correct mean values for the evaluated nuclear data libraries.

## 5.3 Comparison with evaluated data at 400 keV and 500 keV

For fast-reactor applications, evaluated nuclear data libraries recommend cumulative fission yields at 400 keV (JEFF library) and 500 keV (ENDF/B and JENDL libraries). Those for  $^{235}\text{U}$  are reported in Table 1. In Figure 9, our

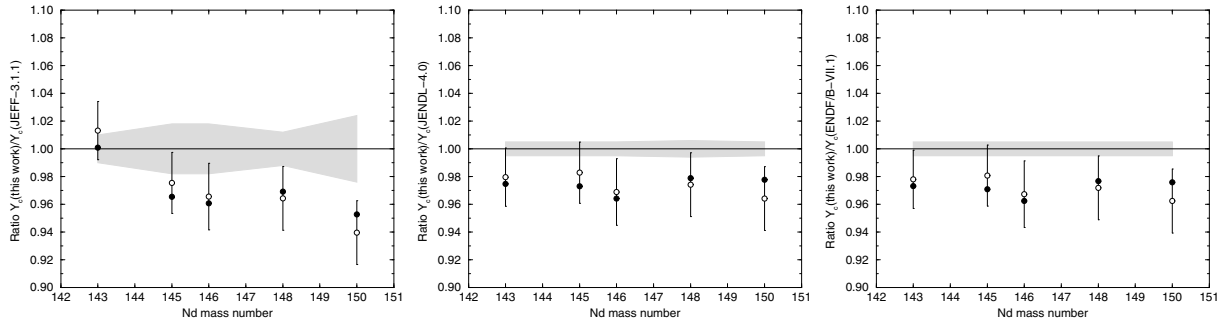


**Fig. 9.** Comparison of the Nd cumulative fission yields obtained in this work and reported in the JEFF, JENDL and ENDF/B evaluated nuclear data libraries. The open circles represent the effective cumulative fission yields deduced from the PROFIL experiments. The black circles are the cumulative fission yields at 400 keV (for the JEFF library) and 500 keV (for the ENDF/B and JENDL libraries) also deduced from the PROFIL results, but they account for a neutron spectrum average correction calculated with the GEF code (Eq. (17)).

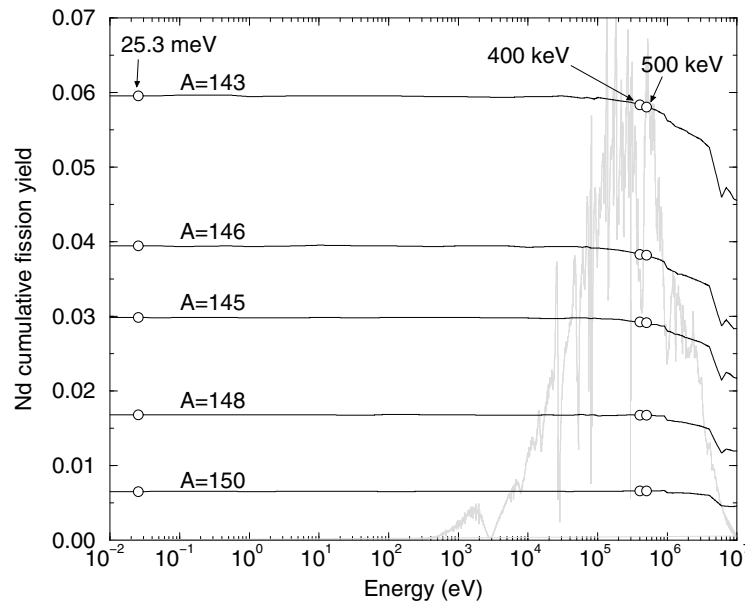


**Fig. 10.** Energy dependence of the Nd cumulative fission yields for  $^{235}\text{U}$  calculated with the GEF code. The GEF results have been normalized at the thermal energy (25.3 meV) with the thermal fission yield recommended in the JEFF-3.1.1 library. They are compared to a neutron spectrum, in arbitrary units, representative of the PROFIL experiments.

effective values for  $^{143}\text{Nd}$ ,  $^{145}\text{Nd}$ ,  $^{146}\text{Nd}$ ,  $^{148}\text{Nd}$  and  $^{150}\text{Nd}$  are compared with values recommended in the JEFF, ENDF/B and JENDL libraries. For JEFF-3.1.1, the decreasing trend with the Nd mass number explains the behavior of the calculated-to-experimental ratios shown in Figures 1 and 5. The cumulative fission yield from the PROFIL experiments are in better agreement with JENDL-4.0 and ENDF/B-VII.1. A systematic bias close to 2% is observed, meaning that the relative uncertainties of 0.5% quoted in the Japanese and US libraries are underestimated.

In the evaluated libraries, the cumulative fission yields for fast neutrons are given at 400 keV or 500 keV, while any effect of neutron energy on fission yields is accounted for during the evaluation procedure. In reference [26], Maecck indicates that this effect can be significant for different positions in a same reactor, without providing an order of magnitude estimate of this effect for the fission yields measured in the EBR-II reactor. In the present work, the

variation of fission yields with the neutron energy was investigated with the GEF code. The code is able to provide systematics for fission yields as a function of the energy for a large number of fissile systems. Preliminary results obtained for the  $^{235}\text{U}(n,f)$  reaction are shown in Figure 10. The results from GEF were normalized at the thermal energy by using the cumulative fission yields of JEFF-3.1.1. The normalization factors range from 1.08 (for  $^{143}\text{Nd}$ ) to 0.6 (for  $^{150}\text{Nd}$ ). The comparison with a fast-neutron spectrum representative of the PROFIL experiments shows the smooth variation of the fission yields in the energy range of interest for fast-reactor applications (around 400 keV and 500 keV). Table 8 reports the normalized cumulative fission yields  $Y_{cg}(^A\text{Nd}, E)$  calculated with GEF at two energies and the effective cumulative fission yields  $\bar{Y}_{cg}(^A\text{Nd})$  calculated with equation (2). Then, the effect of the energy dependence of the fission yields can be estimated with the ratio:

**Table 8.** Results calculated with the GEF code after normalization to the thermal fission yields of JEFF-3.1.1. Columns (a) and (b) give the cumulative fission yields calculated at 400 keV and 500 keV. The column (c) contains the fission yields from GEF weighted by the uranium fission rate calculated for the  $^{235}\text{U}$  samples in the PROFIL experiments. The last two columns give the neutron spectrum average correction defined as the ratios of the fission yields at 400 keV and 500 keV to the effective fission yield.

Nd isotopes	Fission yield $Y_{cG}(^A\text{Nd}, E)$		Effective fission yield $\bar{Y}_{cG}(^A\text{Nd})$ (c)	Correction $\Delta_\phi(E)$	
	$E = 400$ keV (a)	$E = 500$ keV (b)		$E = 400$ keV (a)/(c)	$E = 500$ keV (b)/(c)
$^{143}\text{Nd}$	0.05836	0.05803	0.05867	0.995	0.989
$^{145}\text{Nd}$	0.03831	0.03822	0.03871	0.990	0.987
$^{146}\text{Nd}$	0.02925	0.02917	0.02939	0.995	0.993
$^{148}\text{Nd}$	0.01674	0.01674	0.01665	1.005	1.005
$^{150}\text{Nd}$	0.00663	0.00663	0.00654	1.014	1.014

$$\Delta_\phi(E) = \frac{Y_{cG}(^A\text{Nd}, E)}{\bar{Y}_{cG}(^A\text{Nd})}. \quad (17)$$

In the case of the PROFIL experiments, such a neutron spectrum average correction lies between 0.5% and 1.4%. For each Nd isotope, we also observe that the obtained correction varies slowly with the neutron energy, between 400 keV and 500 keV.

The calculated corrections  $\Delta_\phi(E)$  reported in Table 8 were applied on the effective fission yields  $\langle \bar{Y}_c(^A\text{Nd}) \rangle$  given in Section 5.1 as follow:

$$Y_c(^A\text{Nd}, E) = \Delta_\phi(E) \langle \bar{Y}_c(^A\text{Nd}) \rangle, \quad (18)$$

in order to provide an estimate of  $Y_c(^A\text{Nd}, E)$  at  $E = 400$  keV:

$$Y_c(^{143}\text{Nd}) \simeq 0.0558,$$

$$Y_c(^{145}\text{Nd}) \simeq 0.0367,$$

$$Y_c(^{146}\text{Nd}) \simeq 0.0281,$$

$$Y_c(^{148}\text{Nd}) \simeq 0.0164,$$

$$Y_c(^{150}\text{Nd}) \simeq 0.0067,$$

and at  $E = 500$  keV:

$$Y_c(^{143}\text{Nd}) \simeq 0.0554,$$

$$Y_c(^{145}\text{Nd}) \simeq 0.0365,$$

$$Y_c(^{146}\text{Nd}) \simeq 0.0281,$$

$$Y_c(^{148}\text{Nd}) \simeq 0.0164,$$

$$Y_c(^{150}\text{Nd}) \simeq 0.0067.$$

The results are reported in Figure 9 (black circle). We observe a slight reduction of the dispersion of the Nd values in the case of the comparison with the JENDL and ENDF/B fission yields. The variation of the fission yields with the neutron energy could also contribute to explain the

PROFIL trends with the Nd mass number obtained with the JEFF library (Figs. 1 and 5). The encouraging results from the GEF code (version 1.7, 2013) are still preliminary and have to be considered with care.

## 6 Conclusion

Fast effective Neodymium cumulative fission yields with realistic uncertainties were deduced from the PROFIL experiments. Final results for  $^{143}\text{Nd}$ ,  $^{145}\text{Nd}$ ,  $^{146}\text{Nd}$ ,  $^{148}\text{Nd}$  and  $^{150}\text{Nd}$  were 0.0561, 0.0370, 0.0283, 0.0164 and 0.0066 respectively. The comparison of our effective values with the fission yields recommended in the US and Japanese libraries (ENDF/B-VII.1 and JENDL-4) confirms that the fission yields available in the JEFF-3.1.1 library need to be revised considering this new information. We also found a remaining systematic bias of 2% with the US and Japanese libraries. This bias could indicate that the cumulative fission yield for  $^{148}\text{Nd}$  is overestimated in the international libraries. Such a result is difficult to confirm with the PROFIL experiments because the final uncertainty attached to each of the effective fission yields lies between 2.1% and 2.4%.

The final uncertainty includes the contribution of the fluence scaling uncertainty, which is close to 2%. This well-known source of uncertainty mainly depends on the accuracy of the  $^{235}\text{U}(n,f)$  reaction. The contribution of the uncertainties on the Nd capture cross-sections was also quantified. The magnitude of such a contribution is low (<1%), confirming statements found in previous works. We also report for the first time the impact of the energy dependence of the cumulative fission yields that smoothly decrease in the fast-energy range. The GEF code was used to provide neutron spectrum average corrections ranging from 0.5% to 1.4%. According to these calculations, the neutron spectrum average correction seems to be rather small in the case of the PROFIL experiments.

The GEF calculations have provided encouraging results for future evaluation works. However, this preliminary result has to be confirmed by using an improved version of the code over the seven other fissile systems

measured during the PROFIL experiments ( $^{238}\text{U}$ ,  $^{238}\text{Pu}$ ,  $^{239}\text{Pu}$ ,  $^{240}\text{Pu}$ ,  $^{241}\text{Pu}$ ,  $^{242}\text{Pu}$  and  $^{241}\text{Am}$ ). Such a work is in progress within the frame of the JEFF project.

## References

1. IAEA, Fission product nuclear data, Technical document IAEA-213, 1977
2. OECD, Fission product nuclear data, Technical document NEA/NSC/DOC(92)9, 1992
3. M.B. Chadwick et al., ENDF/B-VII.1 nuclear data for science and technology: cross sections, covariances, fission product yields and decay data, Nucl. Data Sheets **112**, 2887 (2011)
4. K. Shibata et al., JENDL-4.0: a new library for nuclear science and engineering, J. Nucl. Sci. Technol. **48**, 1 (2011)
5. M.A. Kellett et al., The JEFF-3.1/-3.1.1 radioactive decay data and fission yields sub-libraries, Technical document, JEFF report 20, 2009
6. G. Rimpault et al., The ERANOS code and data system for fast reactor neutronic analyses, in *Proc. Int. Conf. PHYSOR 2002, Seoul, Korea* (2002)
7. J.M. Ruggieri et al., ERANOS 2.1: the international code system for GEN-IV fast reactor analysis, in *Proc. Int. Congress on Advances in Nuclear Power Plants, ICAPP06, Reno, USA* (2006)
8. J. Tommasi et al., Analysis of sample irradiation experiments in PHENIX for JEFF-3.0 nuclear data validation, Nucl. Sci. Eng. **154**, 119 (2006)
9. J. Tommasi et al., Analysis of the PROFIL and PROFIL-2 sample irradiation experiments in PHENIX for JEFF-3.1 nuclear data validation, Nucl. Sci. Eng. **160**, 232 (2008)
10. A. Santamarina et al., The JEFF-3.1.1 Nuclear Data Library, Technical document, JEFF report 22, 2009
11. A. Gandini, J. Nucl. Energy **21**, 755 (1967)
12. K.-H. Schmidt et al., General Description of Fission Observables, JEFF Report 24, NEA Data Bank, 2014
13. K.-H. Schmidt et al., General description of fission observables: GEF model code, Nucl. Data Sheets **131**, 107 (2016)
14. R.W. Mills, Fission product yield evaluation, PhD thesis, University of Birmingham, 1995
15. A.R. Date, A.L. Gray, Analyst **108**, 159 (1983)
16. E. Privas et al., The use of nuclear data as Nuisance parameters in the integral data assimilation of the PROFIL experiments, Nucl. Sci. Eng. **182**, 377 (2016)
17. A.D. Carlson et al., International evaluation of neutron cross section standards, Nucl. Data Sheets **110**, 3215 (2009)
18. J. Tommasi, private communication, 2007
19. Z.Y. Bao et al., Neutron cross sections for nucleosynthesis studies, At. Data Nucl. Data Tables **76**, 70 (2000)
20. S.F. Mughabghab, *Atlas of Neutron Resonances*, 5th ed. (Elsevier, Amsterdam, 2006)
21. P. Archier et al., CONRAD evaluation code: development status and perspectives, Nucl. Data Sheets **118**, 488 (2014)
22. W. Davies, Absolute measurements of fission yields for  $^{235}\text{U}$  and  $^{239}\text{Pu}$  in the Dounreay fast reactor, Radio. Acta **12**, 174 (1969)
23. F.L. Lisman et al., Fission yields of over 40 stable and long-lived fission products for thermal neutron fissioned  $^{233}\text{U}$ ,  $^{235}\text{U}$ ,  $^{239}\text{Pu}$  and  $^{241}\text{Pu}$  and fast reactor fissioned  $^{235}\text{U}$  and  $^{239}\text{Pu}$ , Nucl. Sci. Eng. **42**, 191 (1970)
24. M. Robin et al., The importance of fission product nuclear data in burnup determination, in *Proc. Int. Conf. on Chemical and Nuclear Data, Canterbury, UK* (1973)
25. L. Koch, Systematics of fast cumulative fission yields, Radio. Acta **29**, 61 (1981)
26. W.J. Maeck, Fast reactor fission yields for  $^{233}\text{U}$ ,  $^{235}\text{U}$ ,  $^{238}\text{U}$  and  $^{239}\text{Pu}$ , and recommendations for the determination of burnup on FBR mixed oxide fuels, in *Proc. Int. Conf. on Nuclear Cross Sections and Technology, Washington, USA* (1975)
27. M. Rajagopalan et al., Mass yields in the fission of Uranium-235 and Plutonium-239 in the neutron spectrum of a gas-cooled fast reactor, Nucl. Sci. Eng. **58**, 414 (1975)
28. W.J. Maeck et al., Revised EBR-II fast-reactor fission yields for  $^{233}\text{U}$ ,  $^{235}\text{U}$  and  $^{238}\text{U}$ , Exxon Nuclear Idaho Company, report ENICO-1091, 1981

**Cite this article as:** Edwin Privas, Gilles Noguere, Jean Tommasi, Cyrille De Saint Jean, Karl-Heinz Schmidt, Robert Mills, Measurements of the effective cumulative fission yields of  $^{143}\text{Nd}$ ,  $^{145}\text{Nd}$ ,  $^{146}\text{Nd}$ ,  $^{148}\text{Nd}$  and  $^{150}\text{Nd}$  for  $^{235}\text{U}$  in the PHENIX fast reactor, EPJ Nuclear Sci. Technol. **2**, 32 (2016)